DOI 10.70286/EOSS-26.01.2026.001.15-23

TRIM, LINEARIZATION AND PID CONTROLLER DESIGN FOR A MULTI-PURPOSE FIXED-WING AIRCRAFT

Mehmet Karahan
Assistant Professor
Electrical and Electronics Engineering Department
TOBB University of Economics and Technology, Ankara, Turkiye

Abstract. Fixed-wing unmanned aerial vehicles (UAVs) can be used for numerous civilian purposes such as passenger transport, cargo transport, crop dusting, forest fire fighting, and aerial photography. This research presents the trim, linearization, and proportional integral derivative (PID) controller design of a fixed-wing aircraft. Modeling and simulation studies were carried out using MATLAB/Simulink. The created model takes elevator, aileron, rudder, and throttle as input and produces angles, angular rates, and position as output. The analyzed simulation studies confirm the success of the modeling and controller design.

Keywords: Trim, Elevator, Aileron, Rudder, Throttle, PID Control, Fixed-Wing Aircraft

Introduction. The first airplanes invented were fixed-wing aircraft [1]. Fixed-wing aircraft are used for both civilian and defense purposes. Fixed-wing aircraft have been produced for nearly 150 years [2]. During this time, their areas of use have increased. Passenger transport, cargo transport, crop dusting, forest fire fighting, aerial photography, and aerobatics are some of the civilian applications of fixed-wing aircraft [3].

The de Havilland Beaver is a fixed-wing aircraft that can be used for purposes such as firefighting, spraying, and passenger transport. Its ability to take on water from the sea and take off from the sea gives it a significant advantage in firefighting operations [4].

In this study, the modeling, trim, linearization, and PID controller design of the de Havilland Beaver fixed-wing aircraft were carried out in the MATLAB Simulink environment. First, the mathematical equations for the aircraft were provided. Then, modeling was performed using MATLAB Simulink software based on these equations. Using this model, simulations of the aircraft's angles, angular velocities, and position were carried out. Subsequently, this aircraft model was linearized and controlled with a PID controller, and its unit step response was analyzed.

Modeling of the Aircraft. This section explains the equations of motion of the de Havilland Beaver fixed-wing aircraft. Then, the Simulink model of the aircraft is given. Figure 1 shows the axes along which the de Havilland Beaver model moves and its angles of rotation [5]. The fixed-wing aircraft is modeled as a rigid body with a constant mass.

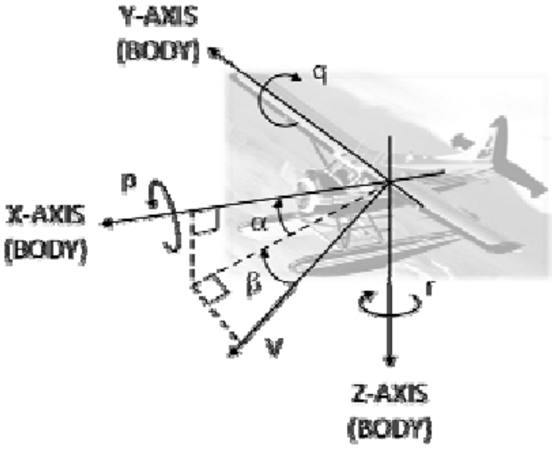

Figure 1: de Havilland Beaver rotation angles and axes

The rotation between the wind axis and the body axis speeds is given in equation (1) [6].

$$\begin{bmatrix} u \\ v \\ w \end{bmatrix} = \begin{bmatrix} \cos\alpha\cos\beta \\ \sin\beta \\ \sin\alpha\cos\beta \end{bmatrix} \tag{1}$$

The reverse transformation equation is given in equation (2).

$$\begin{gathered} V = \sqrt{u^2 + v^2 + w^2} \\ \alpha = \tan^{-1}\frac{w}{u} \\ \beta = \tan^{-1}\frac{v}{\sqrt{u^2 + w^2}} \end{gathered} \tag{2}$$

By taking the derivative of equation (2), the resulting system consisting of three ordinary differential equations can be found to provide analytical explanations for V, α, and β. By taking the derivative of the angle of attack α, equation (3) can be obtained.

$$\dot{\alpha} = \frac{u\dot{w} - w\dot{u}}{u^2 + w^2} \tag{3}$$

If u and w in equation (1) are substituted into equation (3) and rearranged, equation (4) is obtained.

$$\dot{\alpha} = \frac{\dot{w}\cos\alpha - \dot{u}\sin\alpha}{V\cos\beta} \tag{4}$$

The relationships between axial acceleration, gravitational acceleration and angular velocities in the body's reference frame can be given in equation (5) [7].

$$\begin{gathered} \dot{u} = rv - qw - g_0\sin\theta + F_x \\ \dot{v} = -r + pw - g_0\sin\varphi\cos\theta + F_y \\ \dot{w} = q - pv + g_0\cos\varphi\cos\theta + F_z \end{gathered} \tag{5}$$

Equation (6) gives relationships between the normal acceleration n_z and the command actions for the de Havilland Beaver aircraft.

$$n_z = \frac{F_z}{m} = \frac{1}{2}\rho V^2 \left(C_{z0} + C_{z,a}a + C_{z,a^3}a + C_{z,q}\frac{qc}{V} + C_{z,\delta_e}\delta_e + C_{z,\delta_e\beta^2}\delta_e\beta^2\right) \tag{6}$$

Thus, considering equation (5), equation (6) could be rewritten as in equation (7).

$$\dot{a} = \frac{(qu - pv + g_0 \cos\varphi\cos\theta + n_z)\cos\alpha)}{V\cos\beta} - \frac{(rv - qw - g_0\sin\theta + n_z)\sin\alpha)}{V\cos\beta} \quad (7)$$

Next, substituting equation (1), we can get the latest expression for the angle of attack ordinary differential equation (ODE).

$$\dot{a} = \frac{1}{V\cos\beta}\{[V(q\cos\alpha\cos\beta - p\sin\beta) + n_z + g_0\cos\varphi\cos\theta]\cos\alpha - [V(r\sin\beta - q\sin\alpha\cos\beta) - g_0\sin\theta + n_x]\sin\alpha\} \quad (8)$$

Simulations. This section presents the Simulink model of the de Havilland Beaver aircraft and simulations related to this model. Simulations of rotational rates p, q, and r are provided. Simulations of rotation angles phi, theta, and psi are presented. Simulations of the aircraft's movements along the x, y, and h (height) axes are shown. Simulations of the angle of attack (α) and bank angle (β) are given. Finally, the step response of the linearized aircraft model is presented. Simulink model of the De Havilland Beaver aircraft is given in Figure 2.

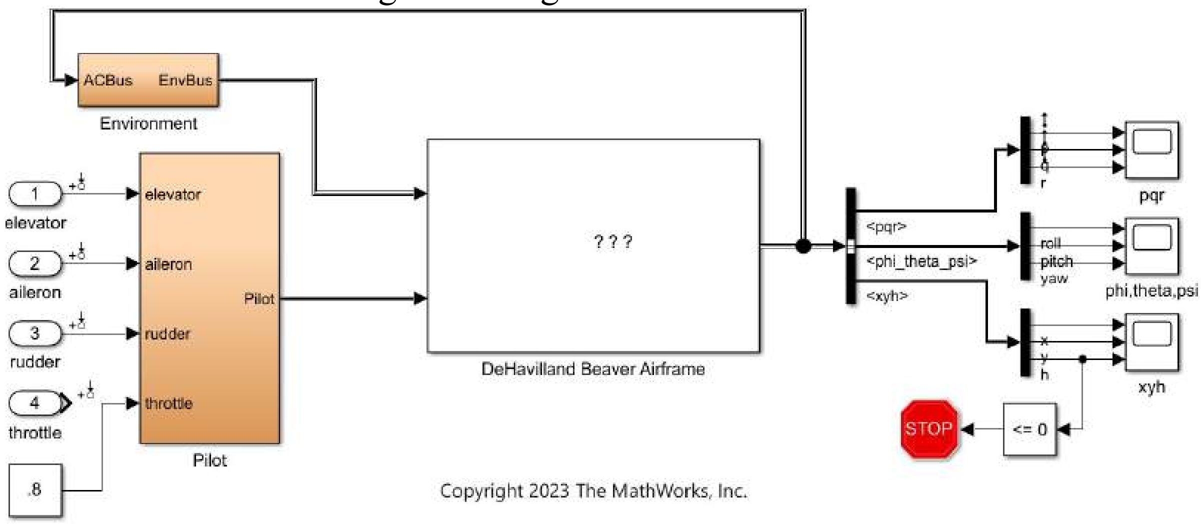

Figure 2: Simulink model of the de Havilland Beaver aircraft.

Figure 3 shows the simulations of the p, q, and r angular velocity components.

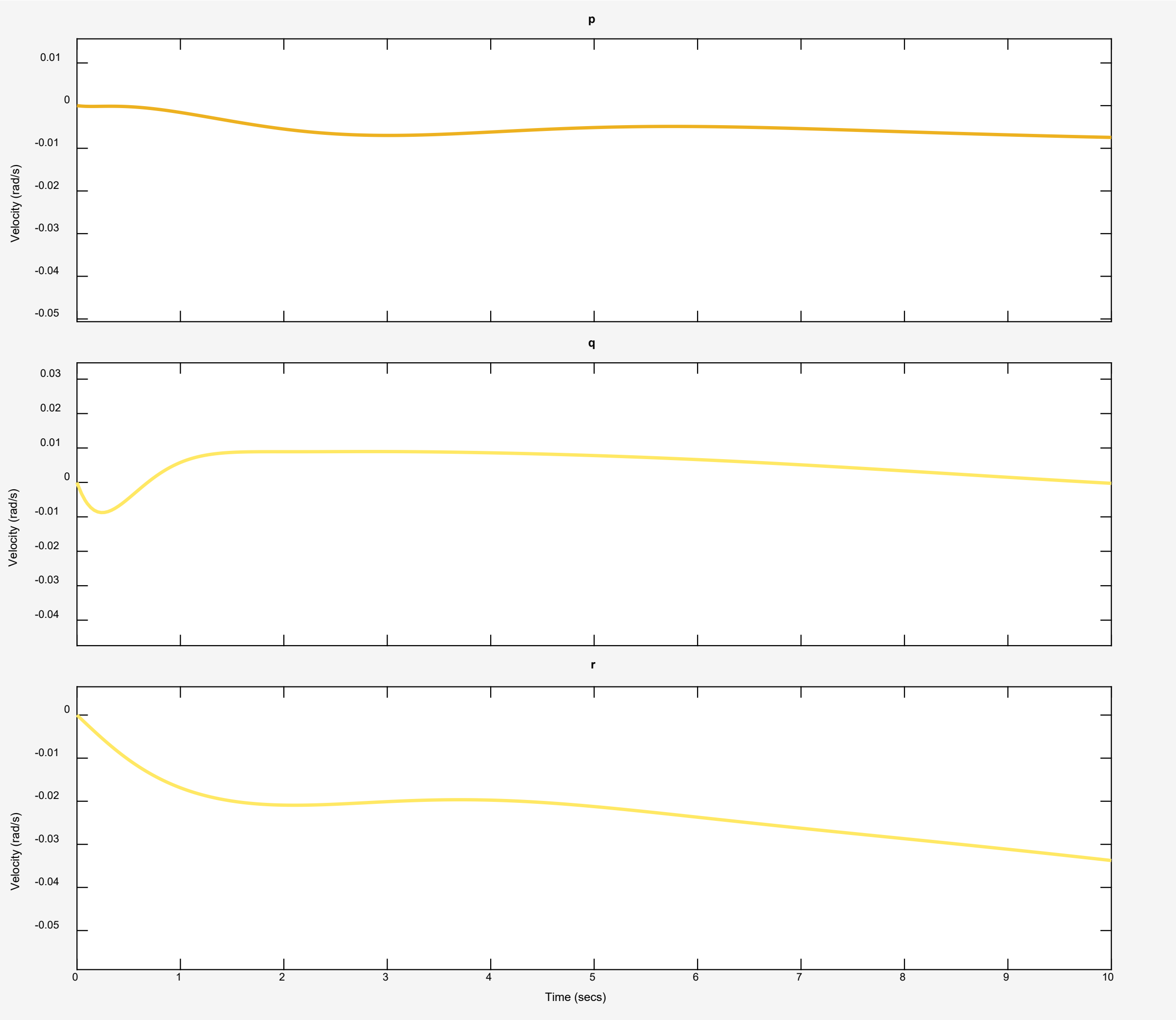

Figure 3: Simulations of the p, q, and r rates.

Figure 4 shows the simulations of the roll, pitch, and yaw angles.

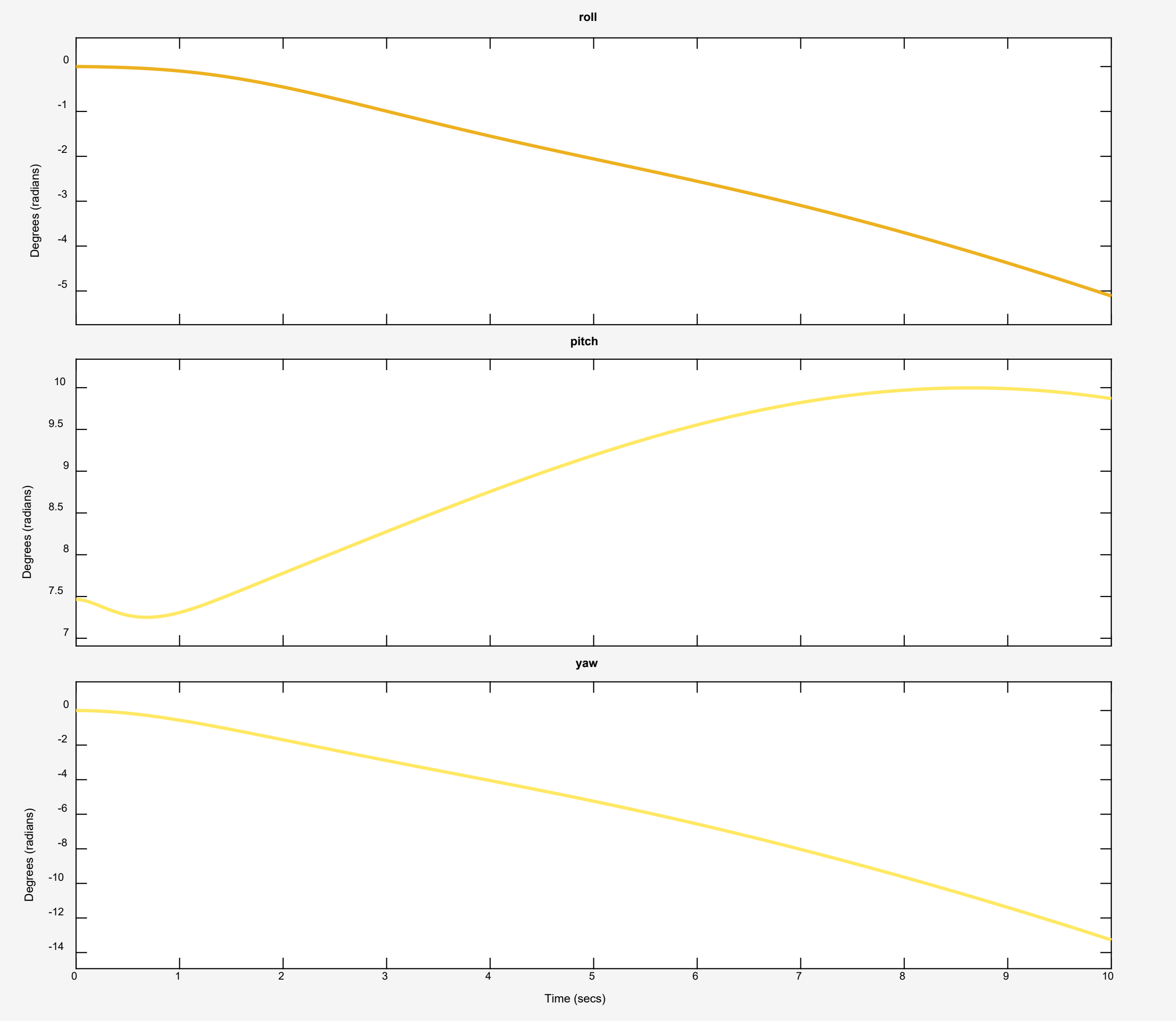

Figure 4: Simulations of the roll, pitch, and yaw angles.

Figure 5 presents the simulations of the movements in the x, y, and h axes.

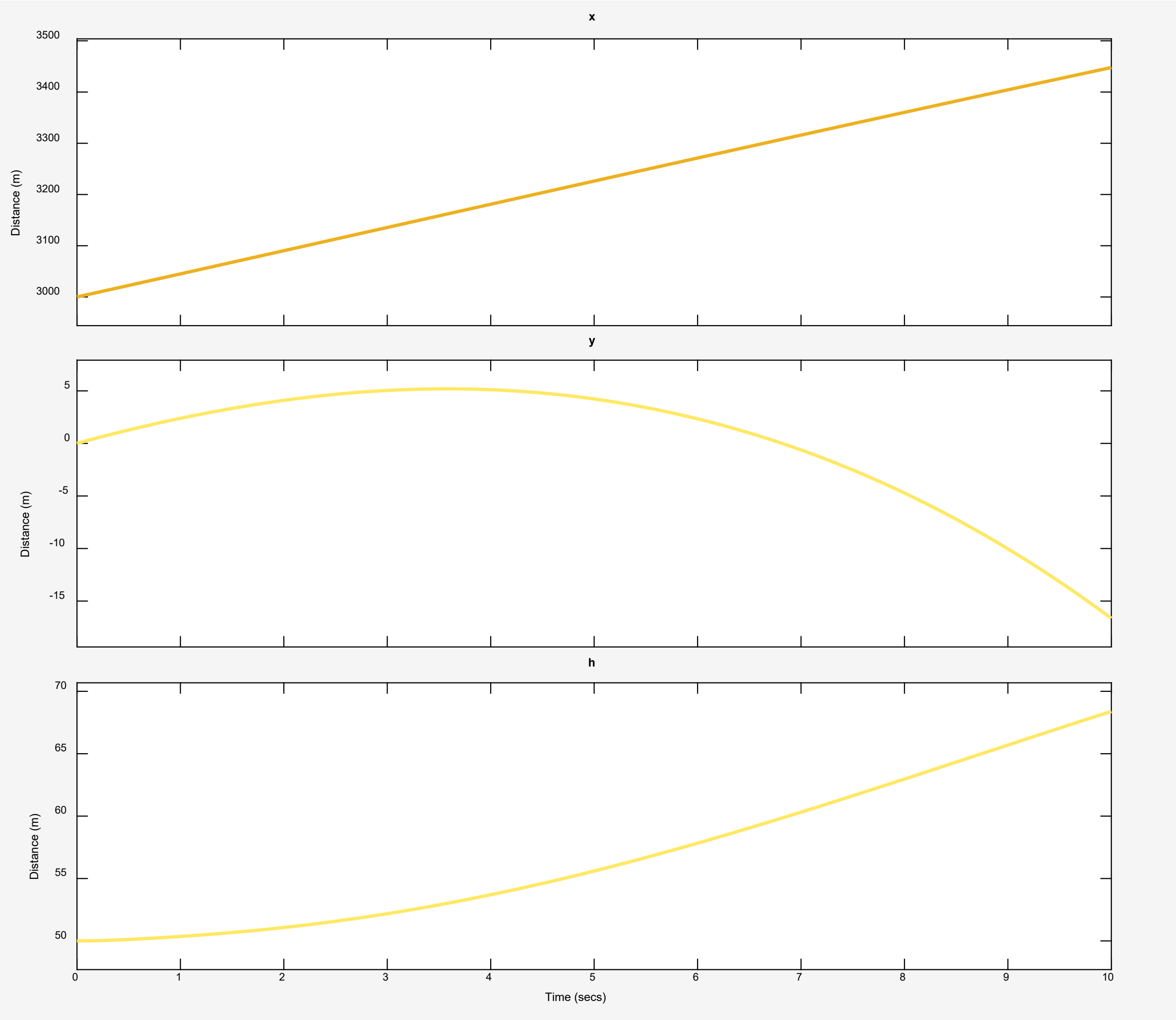

Figure 5: Simulations of the movements in the x, y, and h axes.

Figure 6 represents the simulations of the angle of attack (α) and bank angle (β).

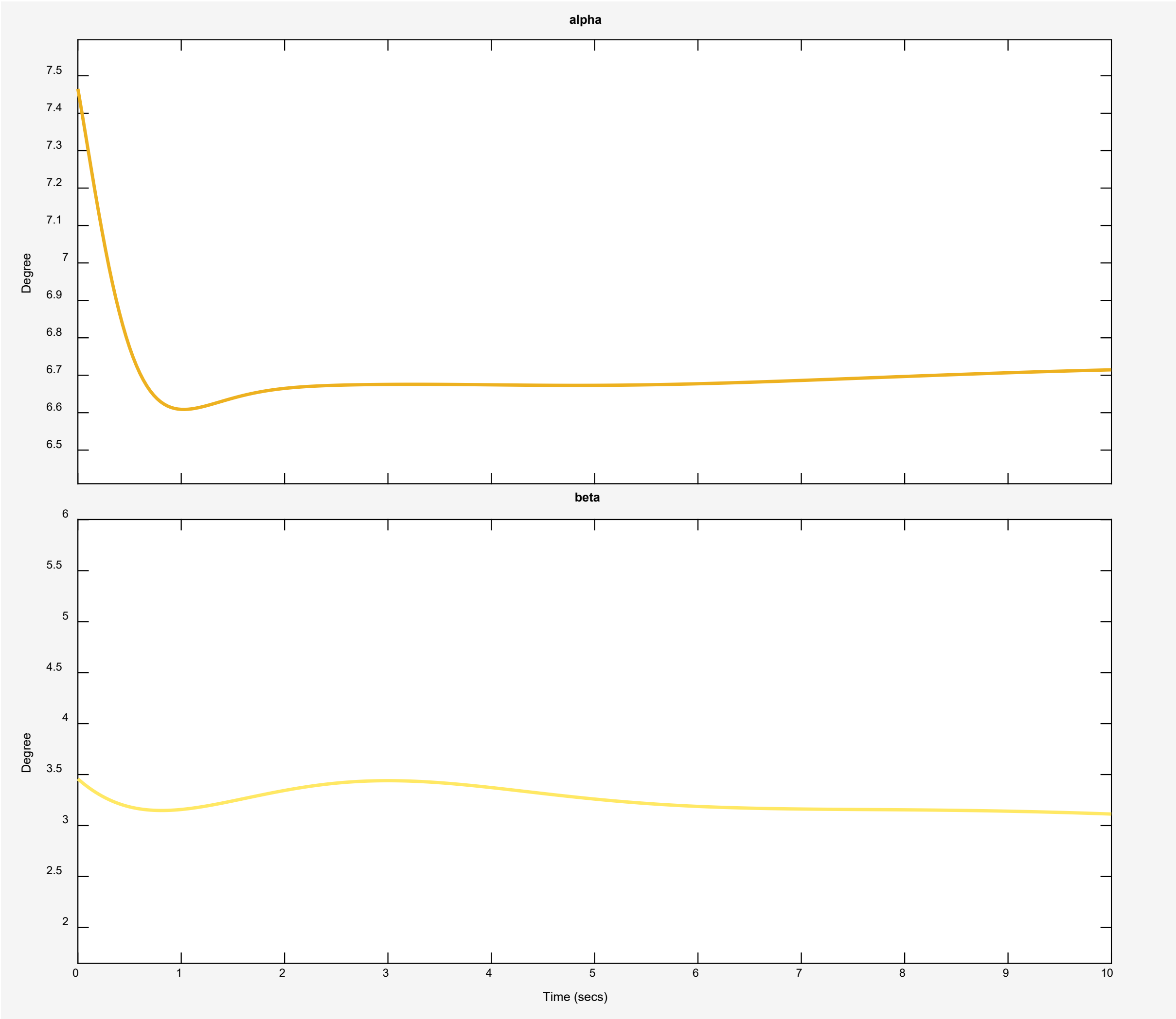

Figure 6: Simulations of the angle of attack (α) and bank angle (β).

When simulations are analyzed, it is clear that the plane is turning as well as descending. The controller design was implemented using Control System Designer. The controller coefficients were adjusted using the PID Tuning graphical tuning method. MATLAB's Graphical User Interface allows for the optimization of PID controller coefficients [8]. Due to its simple structure and easily adjustable coefficients, PID controllers are the most widely used type of controller in industry [9], [10]. The block diagram created in Simulink for the linearized model is shown in Figure 7.

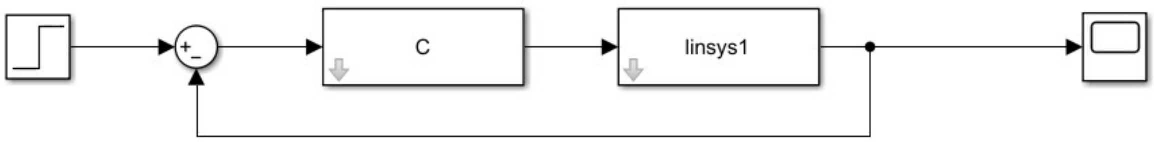

Figure 7: Simulink block scheme of the linearized model.

The unit step response of this linearized model was then examined. Figure 8 shows the step response of the linearized aircraft model. When the graph is examined, it is observed that the linearized model successfully follows the unit step response and does not exhibit steady-state error.

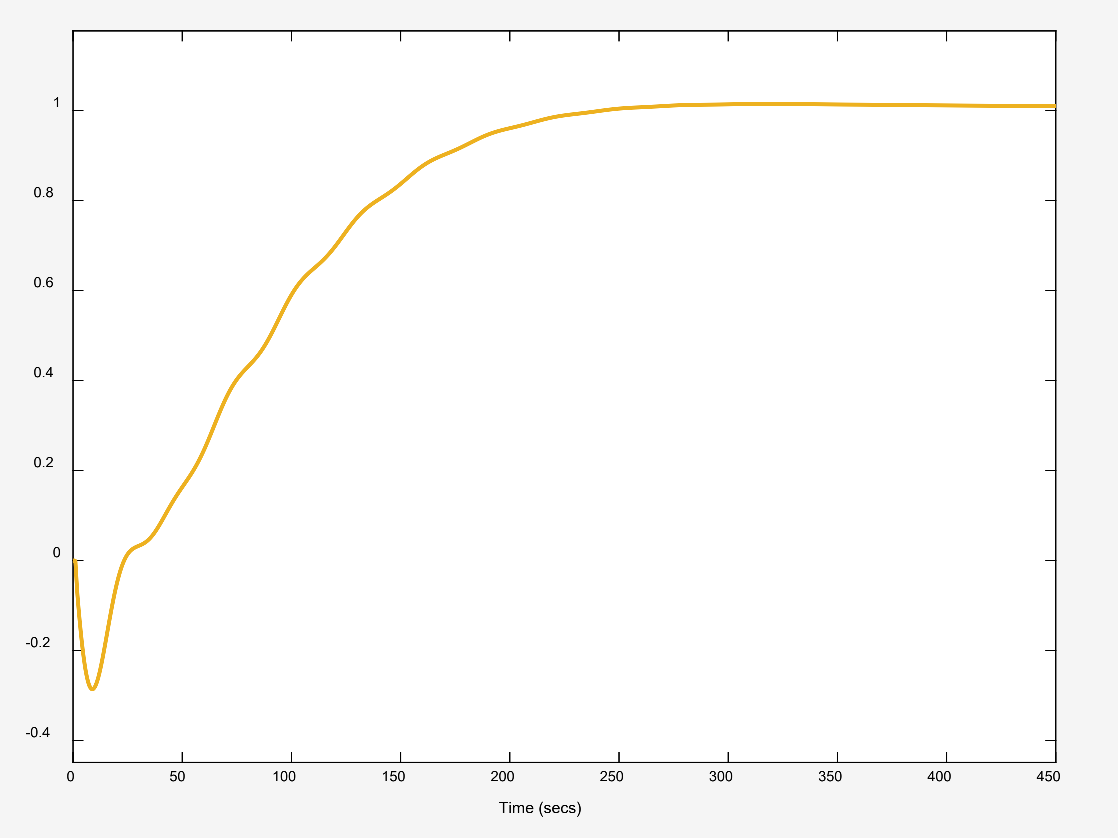

Figure 8: Step response of the linearized aircraft model.

Conclusions. In this study, a de Havilland Beaver fixed-wing aircraft was modeled using MATLAB Simulink. Simulations of rotational rates, rotation angles, movements along the x, y, and h axes, angle of attack (α), and bank angle (β) were then performed. Subsequently, the model was linearized to design a PID controller. A unit step reference tracking simulation was conducted for the designed PID controller. It was observed that the PID controller successfully tracked the unit step reference without steady-state error.

References

1. Petrescu, R. V., Aversa, R., Akash, B., Bucinell, R., Apicella, A., & Petrescu, F. I. (2017). History of aviation-a short review. Journal of Aircraft and Spacecraft Technology, 1(1). URL: https://ssrn.com/abstract=3073974
2. Howard, R. W. (1973). Automatic flight controls in fixed wing aircraft–the first 100 years. The Aeronautical Journal, 77(755), 533-562. DOI: https://doi.org/10.1017/S0001924000041889
3. El-Sayed, A. F. (2016). Classifications of aircrafts and propulsion systems. In Fundamentals of Aircraft and Rocket Propulsion (pp. 1-89). London: Springer London. DOI: https://doi.org/10.1007/978-1-4471-6796-9_1

4. Rossiter, S. (2009). The Immortal Beaver: The World's Greatest Bush Plane. D & M Publishers.
5. Battipede, M., Gili, P., & Lerro, A. (2012, September). Neural networks for air data estimation: Test of neural network simulating real flight instruments. In International Conference on Engineering Applications of Neural Networks (pp. 282-294). Berlin, Heidelberg: Springer Berlin Heidelberg. DOI: https://doi.org/10.1007/978-3-642-32909-8_29
6. Etkin, B., & Reid, L. D. (1995). Dynamics of flight: stability and control. John Wiley & Sons.
7. Rauw, M. O. (2001). FDC 1.2-A Simulink toolbox for flight dynamics and control analysis. Haarlem, The Netherlands.
8. Mohamed, T. L. T., Mohamed, R. H. A., & Mohamed, Z. (2010, March). Development of auto tuning PID controller using graphical user interface (GUI). In 2010 Second International Conference on Computer Engineering and Applications (Vol. 1, pp. 491-495). IEEE. DOI: https://doi.org/10.1109/ICCEA.2010.101
9. Karahan, M. (2025). Development Stages of Quadrotors from Past to Present: A Review. Drones, 9(12), 840. DOI: https://doi.org/10.3390/drones9120840
10. Karahan, M. (2025). Robust Backstepping Control of a Quadrotor Unmanned Aerial Vehicle under Colored Noises. Computers, Materials and Continua, 82(1), 777-798. DOI: https://doi.org/10.32604/cmc.2024.059123